Gradient-driven turbulence in Texas Helimak

Cite as: Phys. Plasmas **29**, 042303 (2022); https://doi.org/10.1063/5.0081036
Submitted: 06 December 2021 • Accepted: 16 March 2022 • Published Online: 05 April 2022

D. L. Toufen, F. A. C. Pereira, Z. O. Guimarães-Filho, et al.

Physics of Plasmas ARTICLE scitation.org/journal/php

Gradient-driven turbulence in Texas Helimak

Cite as: Phys. Plasmas **29**, 042303 (2022); doi: 10.1063/5.0081036
Submitted: 6 December 2021 · Accepted: 16 March 2022 ·
Published Online: 5 April 2022

D. L. Toufen,[1,a)] F. A. C. Pereira,[2,3] Z. O. Guimarães-Filho,[3] I. L. Caldas,[3] and K. W. Gentle[4]

AFFILIATIONS

[1]Federal Institute of Education, Science and Technology of São Paulo—IFSP, 07115-000 Guarulhos, São Paulo, Brazil
[2]Center of Data and Knowledge Integration for Health (CIDACS), Instituto Gonçalo Moniz, Fundação Oswaldo Cruz, 40296-710 Salvador, Bahia, Brazil
[3]Institute of Physics, University of São Paulo, 05315-970 São Paulo, São Paulo, Brazil
[4]Department of Physics and Institute for Fusion Studies, The University of Texas at Austin, Austin, Texas 78712, USA

[a)]**Author to whom correspondence should be addressed:** dennis@ifsp.edu.br

ABSTRACT

We investigate the turbulence level dependence on plasma profiles in experiments in Texas Helimak, a toroidal basic plasma device, with long stable electron cyclotron resonant heating (ECRH) discharges and great flexibility to alter the equilibrium magnetic field. A large set of Langmuir probes is used to obtain the turbulence level and also the plasma radial profiles for several magnetic field intensities with the same safety factor and field line pitch profiles. As a consequence of the ECRH heating, changing the toroidal magnetic field, the equilibrium density profiles are radially displaced. For all the analyzed discharges, with constant magnetic field curvature and shear profiles, we verify that the plasma turbulence has a critical dependence on the equilibrium density profile. Namely, radial regions with negative density radial gradient, i.e., in the opposite direction of the magnetic curvature, present high turbulence level. By properly comparing the turbulence radial profiles with the density peak position, we show that the negative density gradient is the main cause of high amplitude turbulence, in agreement with predictions for ideal interchange modes. Furthermore, intermittence analysis shows that the extreme events (bursts) contribution for the probability density functions (PDFs) is also related to the relative position with respect to the density peak, and that the turbulence level enhancement is likely due to the increase in burst occurrence.

I. INTRODUCTION

In magnetically confined plasmas, electrostatic turbulence observed at the plasma edge limits the confinement performance.[1] Several investigations have predicted the dependence of this electrostatic turbulence on the equilibrium profiles,[2–5] notable the density gradient at the plasma edge.[6,7] However, despite the progress that has been obtained in the observation of this dependence, better measurements of spatial equilibrium profiles and fluctuation characteristics are still necessary to validate models that explain this dependence.[6,8–10]

Meanwhile, electrostatic plasma turbulence and its driven instabilities have already been investigated in basic plasma machines such as Blaamann,[2] Texas Helimak,[11] Large Plasma Device (LAPD),[12] and toroidal plasma experiment (TORPEX).[8,9] Investigations in TORPEX, with consequences for basic plasma machines, describe three possible turbulence patterns: an ideal interchange mode regime, a resistive interchange mode regime, and a drift-wave regime.[13] LAPD discharges were used to identify and describe the gradient-driven drift coupling mode instability.[14,15] Complementary, the Tokamak Chauffage Alfvén Brésilien (TCABR) was configured to perform a basic plasma experiment, namely, to study turbulence in an experiment without plasma current.[7] In this TCABR experiment, high turbulence level was observed for the gradient in the plasma density profile in the opposite direction of the magnetic curvature.

Basic plasma machines have some advantages to investigate plasma turbulence:[9,16] long, stable, and very reproducible discharges; large Langmuir probe distribution through the cold plasma; simple set-ups for changing external parameters like magnetic fields, imposed bias voltage, gas element, and low plasma pressure. These results help to understand the plasma confinement in tokamaks.

The Helimak is a simple toroidal plasma configuration with a magnetohydrodynamic equilibrium[17] and has been used for experimental studies of magnetic plasma confinement.[8,11,18] This device has been proposed to investigate low-frequency gradient-driven instabilities and their routes to turbulence in the presence of magnetic field curvature and shear. The Helimak can be approximately described by an one-dimensional equilibrium in a cylindrical slab geometry,[16] which simplifies the modeling of the observation.

Electrostatic turbulence in Texas Helimak has been investigated to better understand transport,[19,20] waves,[21] and bursts.[22–27] The stability of Texas Helimak discharges allows to vary largely its plasma

parameters. One of these parameters is the toroidal coils electric current, which creates the equilibrium toroidal magnetic field, B_T. Once the achieved density profile is theoretically related to B_T by the electron cyclotron resonance heating (ECRH), it is expected that, by changing B_T, the heating wave resonance and density radial profiles are radially displaced. Thus, by altering the coil current in Texas Helimak, this well-known relation allows to change B_T and modify plasma density equilibrium profiles.

Texas Helimak is a suitable machine to make direct measurements to confirm electrostatic turbulence dependence on the radial density gradient profile, due to the flexibility to change the radial density profile, while keeping other plasma parameters and measuring turbulence along all radial positions. Additionally, the Helimak's lower temperatures and pressures allow for the extensive use of Langmuir probes that give accurate simultaneous measurements of many key plasma parameters profiles. Thus, these measurements could complement contributions that characterize electrostatic plasma turbulence in other machines.[9,12]

In the Texas Helimak experiments analyzed here, the magnetic field line pitch radial profile (the ratio between the vertical and toroidal magnetic fields) can be configurated to remain constant for all imposed coil currents once the proportionality of vertical and toroidal coil currents is controlled by a resistor. Therefore, this configuration permits to distinguish the influence of magnetic and density profiles allowing an overall investigation of the electrostatic plasma turbulence. Moreover, changing the total current through the coils changes only the radial placement of the density maximum without strongly affecting any other plasma quantities. In fact, this property is essential to our analysis reported in this article.

In this work, we configure the Texas Helimak discharges to shift density profiles keeping safety factor and density profiles shape unchanged. Then, we use this setup to experimentally observe the turbulence increase induced by a negative density gradient, in the opposite direction of the magnetic curvature, confirming this gradient as the main energy source or cause of the turbulence. Furthermore, intermittence analysis indicates that this turbulence increase is related to the enhancement of extreme events (bursts) in this region.

In Sec. II, we review the experimental setup. In Sec. III, we present the plasma equilibrium profiles and their dependence with coil field current. In Sec. IV, we show the turbulence basic characteristics and in Sec. V, the results for the relation between equilibrium and turbulence profiles. In Sec. VI, we present the conclusion.

II. EXPERIMENTAL SETUP

A. Texas Helimak

The experiments reported in this work were performed at Texas Helimak[28] in the University of Texas at Austin. This machine has a vacuum vessel with a rectangular cross section of external radius $R_{external} = 1.6$ m, internal radius $R_{internal} = 0.6$ m, and height $= 2$ m. Texas Helimak has a helical magnetic field, shown in Fig. 1, with curvature and shear, which is the result of the combination between the toroidal and the small vertical field. Toroidal and vertical sets of coils share the same electric source, differing only by a resistor that is connected in series with the vertical coils. This common source allows to change the toroidal magnetic field magnitude and keep the connection length profile constant by changing proportionally the toroidal and vertical coils currents. The Helimak magnetic connection lengths are long enough to neglect the boundary effects, becoming an approach to

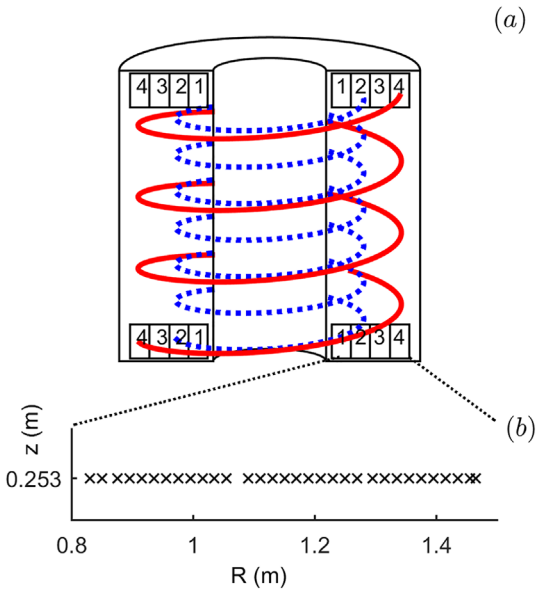

FIG. 1. (a) Schematic representation of Texas Helimak vacuum vessel showing two examples of helicoidal magnetic field lines (R = 1.0 m in dotted blue and 1.4 m in solid red) and the four sets of bias plates. (b) Position of the radially distributed Langmuir probes considered in this work.

a sheared cylindrical slab geometry.[29] Most of the magnetic field lines start and terminate into four sets of four plates located at 180° apart at the top and the bottom parts of the machine. These plates support the Langmuir probes and can be used to apply external electric potentials (bias) to change the radial electric field profile.[20]

The Texas Helimak Argon plasma considered in this work has an average density of $\langle n \rangle = 1 \times 10^{16}\ \mathrm{m}^{-3}$. Electron collision frequency is $\upsilon_{ee} \leq 2 \times 10^5\ (\mathrm{s}^{-1})$. Sound and diamagnetic drift velocities are respectably of the order of $c_s = 5 \times 10^3\ (\mathrm{m/s})$ and $v_{de} = 10^3\ (\mathrm{m/s})$.

The experiments considered in this work analyze turbulence in a set of discharges with five different toroidal coil current values ($I_C = 750$, 800, 900, 1000, and 1100 A). The discharges were performed with argon gas at 10^{-5} Torr, heated by 6 kW ECRH at fundamental 2.45 GHz inserted by a window located on the inner side of the vacuum vessel. In a grounded operation discharge, with all the plates connected to the vessel ground, equilibrium electric potential results from the sheath boundary conditions, creating a vertical E × B sheared flows.[28] For all presented discharges, the total duration is up to 20 s with the plasma in almost stationary steady state of which 10 s are considered for fluctuation analysis described in this work.

The results presented in this work were obtained by a large array of electrostatic probes mounted at the plates in the bottom part of the machine, see Fig. 1. The measured saturation current fluctuations analyzed was mainly acquired by a digitizer with 96 channels and 500 kS/s of sample rate, connected to the probes shown in Fig. 1(b).

B. Toroidal magnetic field and plasma heating

In Texas Helimak, the toroidal magnetic field (B_T) can be modified by changing the toroidal coil current (I_C). This field can be

considered independent of the toroidal angle with a radial dependence $B_T \propto \frac{I_C}{R}$, where R is the radial position. Therefore, changing I_C shifts the B_T radial profiles. As the heating power is always the same, the localized heating induced by the microwaves is linked with B_T, because it depends on the resonance position between the frequency of the microwave source and the electron cyclotronic frequency ($w_C = \frac{eB}{m_e}$).[30] It follows that there is a direct relation between the radial position where the maximum heating occurs (R_{MH}) and the coils current: $R_{MH} \propto I_C$.

In the analyzed experiments, by controlling B_T through I_C, we obtain discharges with plasma density radial profiles with the same shape but shifted radial positions. Even varying I_C, the safety factor profile remains constant once it is determined by the ratio between the toroidal and vertical magnetic field components: $q = \frac{h}{pitch} \propto \frac{1}{R}$. Therefore, the magnetic shear, $s = \frac{1}{R}\frac{dq}{dR}$, remains constant too for all I_C values.

C. Data analyses

The data that support the findings of this study, Texas Helimak discharges from 150 223 006 to 150 226 013, are available from the corresponding author upon reasonable request.

Equilibrium and turbulent values presented in this work were computed by dividing the total acquired time series into 100 intervals and calculating the aimed values of each subseries. Then, means over these 100 subseries values are adopted as the better estimation of those values, being their standard deviation of the mean adopted as an estimative of the means uncertainty.

The presented temperature profiles are obtained by imposing ramp potential at the probes and analyzing $I \times V$ electric probe curves following the procedure shown in Ref. 24.

III. EQUILIBRIUM PROFILES DEPENDENCE ON THE TOROIDAL MAGNETIC FIELD

The mean value profiles of the ion saturation current ($\langle I_{sat} \rangle$), directly related to the density profiles, were measured for a set of discharges, each one with a different fixed coil field current (I_C). The results are shown in Fig. 2(a). This figure shows clearly that the saturation current profiles shift with the change of the coil current. To compare these profiles with the expected toroidal magnetic field (B_T), we present in Fig. 2(b) the mean I_{sat} values plotted in a grayscale with I_C in the vertical axis. In this figure, we indicate five values of constant B_T in the dashed red lines labeled from 1 (higher) to 5 (lower). Comparing the mean I_{sat} at grayscale with the constant B_T lines, we recognize that the radial profiles of the I_{sat}, therefore the density, are directly related to the B_T values. This result is expected, once the heating depends on the B_T, which imposes the position of maximum heating and density close to number 3 line. The ∇I_{sat} values are presented in Fig. 3 as a function of I_c and R. The dashed lines in this figure indicate values of constant B_T. In Fig. 3, we observe, on the left and right sides of the BT constant dashed line 3, a positive and a negative region density gradient colored in red and blue, respectively. The easy localization of maximum density and gradients radial regions makes possible to better understand the relations between turbulence and equilibrium characteristics of Texas Helimak plasma.

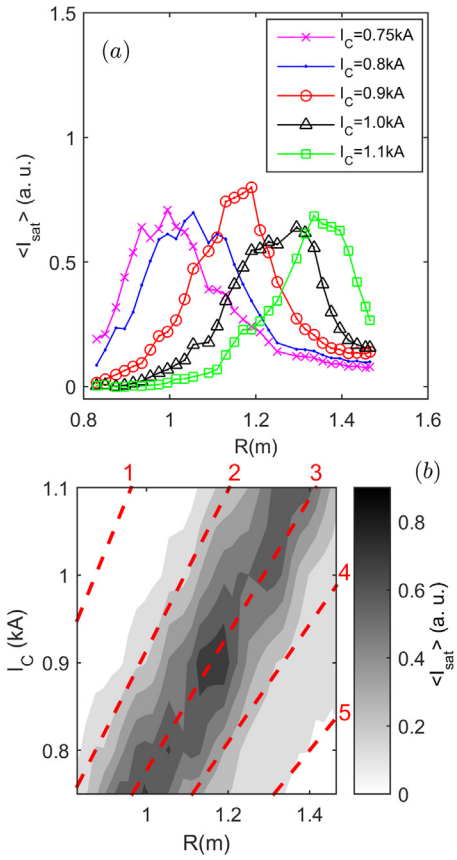

FIG. 2. Mean value of ion saturation current (I_{sat}) as a function of radial position and coil currents (I_C) (a). Same profiles with I_{sat} plotted in a grayscale (b). The dashed red lines indicate five values of magnetic toroidal field (B_T).

Electron temperature profiles are presented in Fig. 4 showing that the temperate profile is also shifted when coil current changes. This is expected once electron temperature should follow the maximum heating radial region.

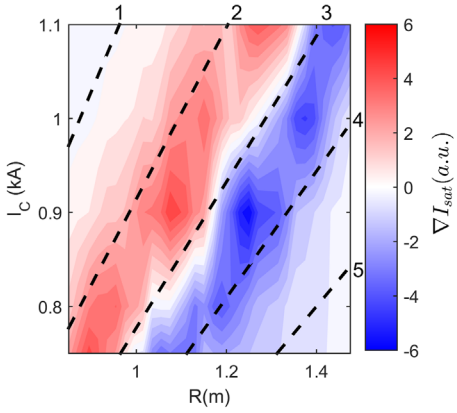

FIG. 3. Radial gradient of mean value of ion saturation current smoothed by a three movable radial positions average. The dashed lines indicate five values of magnetic toroidal field (B_T).

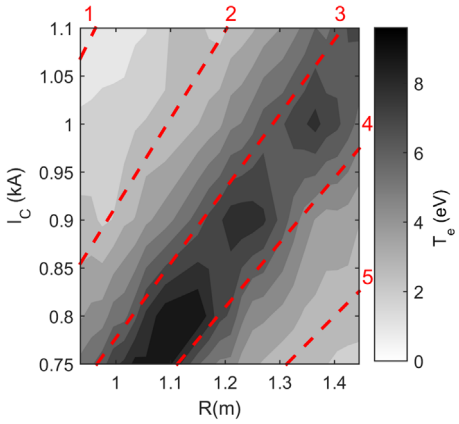

FIG. 4. Electron temperature as a function of radial position and coil currents. The dashed red lines indicate five values of magnetic toroidal field (B_T).

IV. BASIC TURBULENCE

The most basic statistical parameter of the turbulence is the I_{sat} signal standard deviation (σ_{Isat}), which is related to the amplitude of I_{sat} fluctuation. The radial profiles of σ_{Isat} are shown in grayscale in Fig. 5(a). The dashed lines represent the same B_T values shown in the Figs. 2(b) and 3. By observing Fig. 5, we note the direct dependency of I_{sat} fluctuation with B_T. Moreover, we note that the maximum radial position of σ_{Isat} is barely at the right side of the B_T number 3 line. Furthermore, comparing Figs. 3 and 4(a), it is noticeable that σ_{Isat} is high for negative values of ∇I_{sat}, indicating that the turbulence in Texas Helimak is determined by the negative radial gradient of plasma density. For the same turbulence level, σ_{Isat} should be proportional to the $\langle I_{sat}\rangle$, so we compute the density turbulence level by the quotient between σ_{Isat} and $\langle I_{sat}\rangle$, the result is shown in Fig. 5(b).

V. TURBULENCE PATTERNS

Figure 5(b) shows a strong inverse dependence of the turbulence level on the magnetic toroidal field. Additionally, the radial position where turbulence level presents a drastic increase is higher for intense coil field current (I_C). To better show the dependence of turbulence level on B_T, we present the curves in a one-dimensional scheme in Fig. 6. According to Fig. 6, the turbulence level depends on B_T, having higher values for low B_T and lower values for high B_T. Furthermore, the B_T required for the high to the low turbulence level transitions shows a dependence on the coil current. Consequently, the more important parameter to trigger these two turbulence behaviors is in fact the density profile.

The turbulence level dependence with density profile is shown in Fig. 7, where the turbulence level (a), mean (b), and standard deviation (c) saturation current radial profiles are presented as a function of the radial position relative to the maximum saturation current radial position (R_{max}). In Fig. 7, it is clear that the turbulence level is lower on the left side of the R_{max} for every I_c and presents a fast increase for the right side of R_{max}. As these relative positions to the maximum are related to the density gradient, with $\nabla n > 0$ for $R < R_{max}$ and $\nabla n < 0$ for $R > R_{max}$, the turbulence level behavior is strongly related to the density gradient, presenting two regimes of relative amplitude. The high relative turbulence level regime occurs for the negative density gradients, and the low relative amplitude regime occurs for positive density gradients.

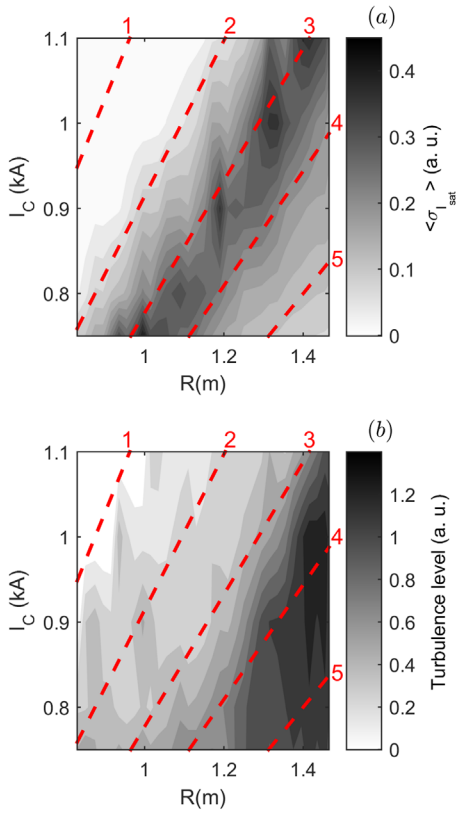

FIG. 5. Ion saturation current fluctuation measured by the standard deviation as a function of radial position and coil currents (a). Saturation current turbulence level as a function of radial position and coil field current (b). The value close to $I_c > 1050$ A and $R < 1$ m is forced to zero once there is no plasma at this region. The dashed red lines indicate five values of magnetic toroidal field (B_T).

In Helimaks, ideal interchange and resistive drift modes have been identified as the source of turbulence.[6,10,13,31] The ideal

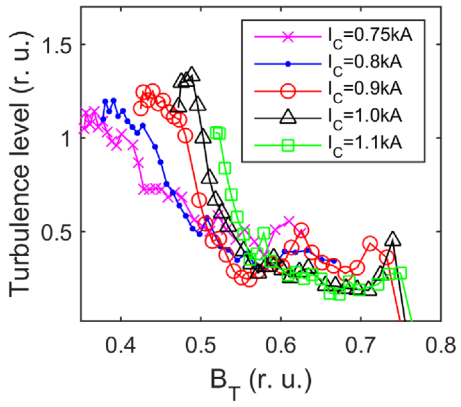

FIG. 6. Saturation current turbulence level as a function of magnetic toroidal field (B_T) for five values of toroidal current.

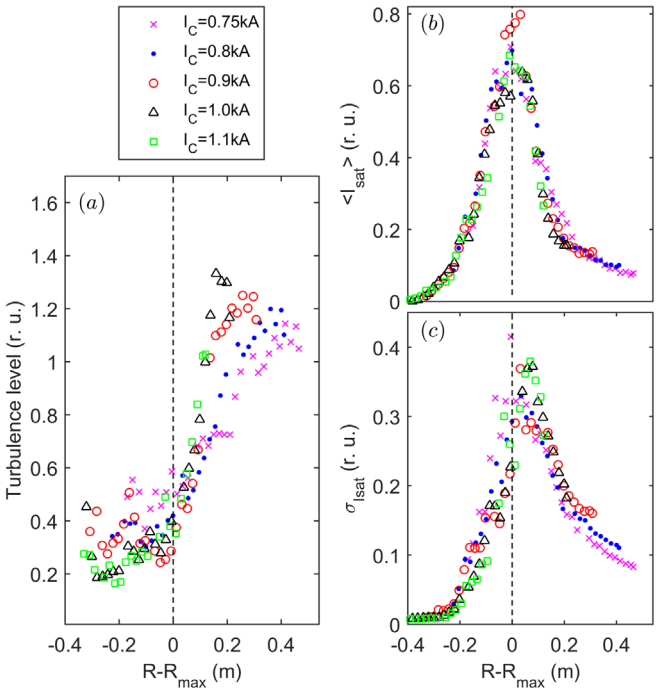

FIG. 7. Turbulence level (a), mean (b), and standard deviation (c) of saturation current as a function of radial position relative to R_{max} for five values of toroidal current. R_{max} is the radial position of the maximum of the mean I_{sat} radial profile (marked as a vertical dashed line).

interchange mode has a wave vector exactly perpendicular to the magnetic field, i.e., a wavenumber parallel to the magnetic field identically equal to zero. Unlike the interchange instability in which all motion is perpendicular to the magnetic field, leading to null parallel wave vector, for drift waves this component has a small non-null value. Assuming a fluid description of plasma, in Ref. 6, the authors derived a dispersion relation for drift waves in Helimaks.

In Ref. 13, the authors analyzed theoretically the plasma instabilities in simple toroidal machines and identified the ideal interchange regime, the resistive interchange regime, and the drift wave regime, the three regimes dominated by distinct plasma instabilities. As an example, they found that drift waves would dominate at the lower collisionality typically seen in TORPEX plasmas.[9]

For the discharges analyzed in our work, at the considered regions with high pitch, the values of the wave vector component parallel to the magnetic field, within reasonable experimental error, is equal to zero. The modes have wavelengths much longer than the size of the device and thus constitute a close experimental approximation to the theoretical ideal interchange mode. Thus, in the discharges analyzed in this work, electrostatic fluctuations should be driven by ideal interchange instability.[31] In fact, this instability requires density gradient and magnetic curvature pointing in the opposite directions, which agrees with our observations of high turbulence level for radial positions higher than R_{max}.

To identify the ideal interchange instability in Texas Helimak discharges, Williams estimates the $\alpha_\perp$ and $\alpha_\parallel$ dimensionless parameters[31] suitable for different instabilities distinction, introduced by Ricci and Rogers.[10,13] For the pitch used in the discharges analyzed here $\alpha_\perp \cong 0.26$ and $\alpha_\parallel \cong 6010$ (Ref. 31, p. 33), characterizing the ideal interchange instability once this instability is favored for $\alpha_\perp < 1$ and $\alpha_\parallel \gg 1$, as predicted in Ref. 13.

To better characterize this increase in turbulence, we investigate the presence of extreme events. The skewness and kurtosis radial profiles as a function of coil currents (Fig. 8) show that in the low field side of the peak radial positions, where the turbulence level increases, the skewness and kurtosis also increase suggesting a bigger contribution of extreme events. Taking the R_{max} as a reference, we show in Fig. 9 probability density functions (PDFs) of the ion saturation current for high field side, $R = R_{max} - 0.15$ cm, (a) and low field side $R = R_{max} + 0.15$ cm (b), of the density peak radial position. The PDFs in the high field side are almost gaussians, while in the low field side, where turbulence increases, present pronounced tail.

A stochastic model for the turbulence was used to estimate the contribution of coherent structures related to bursts for the density fluctuations.[32] The model, also called filtered Poisson process, consists of a pulse train model with a background noise component[27] and has successfully been used in several tokamaks with local density fluctuations measured by different diagnostics[33–35] and also in other Texas Helimak experiments.[27]

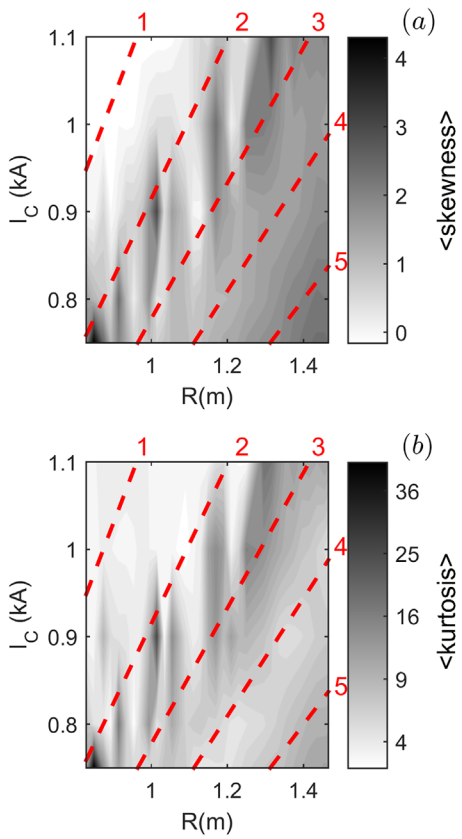

FIG. 8. Ion saturation current skewness (a) and kurtosis (b) as a function of radial position and coil field current. The dashed red lines indicate five values of magnetic toroidal field (B_T).

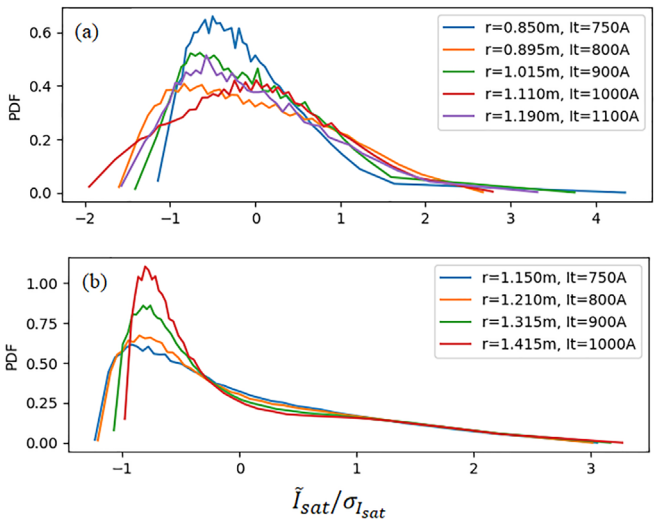

FIG. 9. Ion saturation current PDFs for several coil currents I_c and -0.15 cm (a) $+0.15$ cm (b) of radial position relative to R_{max}. Here, $\sim I_{sat} = I_{sat} - \langle I_{sat} \rangle$ is the fluctuation ion saturation current. These PDFs indicate that turbulence level increase in the low field side by the contribution of extreme events, as suggested by skewness and kurtosis analyses.

The background noise represents incoherent plasma fluctuations and electronic noise contributions and is simulated by adding Gaussian random numbers. The pulses represent the coherent structures and are simulated by considering independent random time occurrences of peaks with the same temporal shape multiplied by random positive amplitudes that follow an exponential distribution, in agreement with experimental observations of the conditional average of the extreme events (bursts) in several machines. Therefore, these pulses are responsible for the asymmetry of the PDFs, and the bursts are related to the high amplitude pulses. A double exponential fit of the conditional average of the bursts is used to determine the pulse temporal shape for the simulation, whose PDF is a gamma distribution.

In this model, the experimental histogram is fitted by a theoretical PDF obtained by a numerical convolution of the background distribution (a normal distribution) and the coherent structures one (a gamma distribution). The background and pulse parameters were determined by using a nonlinear least squares routine.

Model adjusts for two PDFs at $R = R_{max} + 0.25$ cm are shown in Fig. 10. The pulse train model describes well the observed PDFs, and the parameters show that the pulse contribution for the variance in the peak low field side is at least 95%, while almost no pulse contribution is necessary to fit the PDFs at the high field side. On the other hand, the fits also show that in the peak low field side, the pulse contribution for the average is about 75%. This relevant contribution of the pulses helps to understand why the average reduction in the peak low field side is not followed by a proportional reduction in the standard deviation, once due to the pulse temporal shape, their contribution for the average is much less important than the contribution for the standard deviation (and high orders normalized moments, as seen for the skewness and kurtosis).

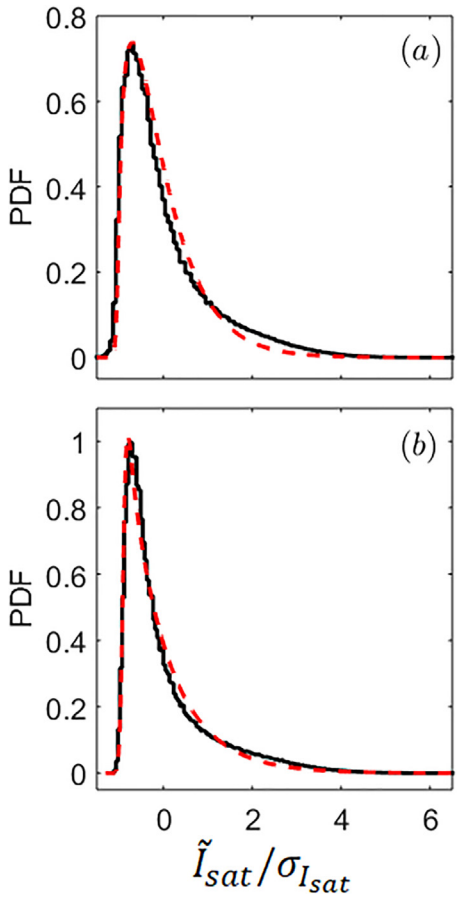

FIG. 10. Model adjusts (red dashed line) of the PDF (black solid line) for Ic = 800 A, R = 1.295 m (a) and Ic = 900 A, R = 1.415 m (b), both of +0.25 cm of relative distance from density peak position, R_{max}. The observed long tail corresponds to the burst contribution in regions where high values of turbulence level are observed.

VI. CONCLUSIONS

Using the capability of Texas Helimak to provide stable discharges for several magnetic field values, we analyze discharges with five coil currents values, which change proportionally toroidal and vertical magnetic fields, keeping the pitch and the safety factor radial profile.

As expected, the density profile depends mainly on the toroidal magnetic field once the resonant heating region changes with magnetic field. Direct observations of turbulence level radial profiles show two regimes of turbulence, with low and high amplitudes. Its transition depends not only on the magnetic field but the coil currents too, leading to that the fundamental dependence of the turbulence regime transition is with the density profile. Taking the maximum density radial position, R_{max}, as a reference, we show that turbulence level increases where $R > R_{max}$ and consequently, where the density gradient is negative.

From this work, we experimentally verify the relation between turbulence and density gradient showing that the high turbulence level

occurs in the region where the gradient density and the magnetic curvature have opposite directions. As in Texas Helimak, the pressure gradient is dominated by the density gradient, our results agree with the prediction for ideal interchange modes.

Intermittence analysis shows that the turbulence level growth at the low field side of the density peak is likely due to the enhancement of the extreme events that are the main contributions for the density fluctuations in this region.

In conclusion, our work confirms that turbulence enhancement in magnetically confined plasmas occurs in the negative density gradient region, Moreover, we show a direct observation that the electrostatic turbulence profile in Texas Helimak is determined by the relative distance with respect to the peak density position.

ACKNOWLEDGMENTS

We would like to acknowledge financial support from the Brazilian agencies: Sao Paulo Research Foundation (FAPESP)-Grant No. 2018/03211-6 and CNPq-Grant Nos. 302665/2017-0, 407299/2018-1, and 312771/2019-3. We also thank L. A. Osorio and M. Zurita for revising the article.

AUTHOR DECLARATIONS

Conflict of Interest

The authors have no conflicts to disclose.

DATA AVAILABILITY

The data that support the findings of this study are available from the corresponding author upon reasonable request.

REFERENCES

[1]C. W. Horton, Jr. and S. Benkadda, *ITER Physics* (World Scientific, 2015).
[2]F. J. Øynes, H. L. Pécseli, and K. Rypdal, Phys. Rev. Lett. **75**, 81 (1995).
[3]W. Horton, *Turbulent Transport in Magnetized Plasmas*, 2nd ed. (World Scientific, 2018).
[4]R. D. Hazeltine and J. D. Meiss, *Plasma Confinement* (Addison-Wesley, Reading, MA, 1992).
[5]R. D. Hazeltine and S. C. Prager, Phys. Today **55**(7), 30–36 (2002).
[6]J. C. Perez and W. Horton, Phys. Plasmas **13**, 032101 (2006).
[7]A. A. Ferreira, M. V. A. P. Heller, and I. L. Caldas, Phys. Plasmas **7**, 3567 (2000).
[8]S. H. Müller, A. Fasoli, B. Labit, M. McGrath, M. Podestà, and F. M. Poli, Phys. Rev. Lett. **93**, 165003 (2004).
[9]A. Fasoli, I. Furno, and P. Ricci, Nat. Phys. **15**, 872 (2019).
[10]B. N. Rogers and P. Ricci, Phys. Rev. Lett. **104**, 225002 (2010).
[11]K. W. Gentle and H. He, Plasma Sci. Technol. **10**, 284 (2008).
[12]T. A. Carter, B. Van Compernolle, and M. J. Poulos, "Advances in fusion-relevant physics on the large plasma device," Technical Report No. IAEA-CN–258 [International Atomic Energy Agency (IAEA), 2018].
[13]P. Ricci and B. N. Rogers, Phys. Rev. Lett. **104**, 145001 (2010).
[14]M. J. Pueschel, P. W. Terry, D. Told, and F. Jenko, Phys. Plasmas **22**, 062105 (2015).
[15]M. J. Pueschel, G. Rossi, D. Told, P. W. Terry, F. Jenko, and T. A. Carter, Plasma Phys. Controlled Fusion **59**, 024006 (2017).
[16]K. W. Gentle, W. L. Rowan, C. B. Williams, and M. W. Brookman, Phys. Plasmas **21**, 092302 (2014).
[17]E. D. Zimmerman and S. C. Luckhardt, J. Fusion Energy **12**, 289 (1993).
[18]K. Rypdal and S. Ratynskaia, Phys. Rev. Lett. **94**, 225002 (2005).
[19]B. Li, B. N. Rogers, P. Ricci, K. W. Gentle, and A. Bhattacharjee, Phys. Rev. E **83**, 056406 (2011).
[20]D. Toufen, Z. Guimarães Filho, I. L. Caldas, F. A. Marcus, and K. Gentle, Phys. Plasmas **19**, 012307 (2012).
[21]D. L. Toufen, Z. O. Guimarães-Filho, I. L. Caldas, J. D. Szezech, S. Lopes, R. L. Viana, and K. W. Gentle, Phys. Plasmas **20**, 022310 (2013).
[22]D. L. Toufen, F. A. C. Pereira, Z. O. Guimarães-Filho, I. L. Caldas, and K. W. Gentle, Phys. Plasmas **21**, 122302 (2014).
[23]F. A. C. Pereira, D. L. Toufen, Z. O. Guimarães-Filho, I. L. Caldas, and K. W. Gentle, Plasma Phys. Controlled Fusion **58**, 054007 (2016).
[24]F. A. C. Pereira, W. A. Hernandez, D. L. Toufen, Z. O. Guimarães-Filho, I. L. Caldas, and K. W. Gentle, Phys. Plasmas **25**, 042301 (2018).
[25]F. A. C. Pereira, I. M. Sokolov, D. L. Toufen, Z. O. Guimarães-Filho, I. L. Caldas, and K. W. Gentle, Phys. Plasmas **26**, 052301 (2019).
[26]T. N. Bernard, E. L. Shi, K. W. Gentle, A. Hakim, G. W. Hammett, T. Stoltzfus-Dueck, and E. I. Taylor, Phys. Plasmas **26**, 042301 (2019).
[27]F. A. C. Pereira, D. L. Toufen, Z. O. Guimarães-Filho, I. L. Caldas, R. L. Viana, and K. W. Gentle, Phys. Plasmas **28**, 032301 (2021).
[28]K. W. Gentle, K. Liao, K. LEE, and W. L. Rowan, Plasma Sci. Technol. **12**, 391 (2010).
[29]S. Luckhardt, "The Helimak: A one dimensional toroidal plasma system," Technical Report No. UCSD-ENG-069 (University of California, San Diego, 1999).
[30]F. Chen, *Introduction to Plasma Physics and Controlled Fusion*, 3rd ed. (Springer, 2015).
[31]C. B. Williams, "Characterization of instability regimes in the Helimak, a simple magnetic torus," Ph.D. thesis (The University of Texas at Austin, 2017).
[32]O. E. Garcia, Phys. Rev. Lett. **108**, 265001 (2012).
[33]A. Theodorsen, O. E. Garcia, R. Kube, B. LaBombard, and J. L. Terry, Nucl. Fusion **57**, 114004 (2017).
[34]R. Kube, A. Theodorsen, O. E. Garcia, D. Brunner, B. LaBombard, and J. L. Terry, J. Plasma Phys. **86**, 905860519 (2020).
[35]A. Bencze, M. Berta, A. Buzás, P. Hacek, J. Krbec, M. Szutyányi, and COMPASS Team, Plasma Phys. Controlled Fusion **61**, 085014 (2019).